



Light stop decays into $Wb\tilde{\chi}_1^0$ near the kinematic threshold



Ramona Gröber^{a,*}, Margarete Mühlleitner^b, Eva Popenda^c, Alexander Wlotzka^b

^a INFN, Sezione di Roma Tre, Via della Vasca Navale 84, I-00146 Roma, Italy

^b Institute for Theoretical Physics, Karlsruhe Institute of Technology, Wolfgang-Gaede Str. 1, D-76128 Karlsruhe, Germany

^c Paul Scherrer Institute, CH-5232 Villigen PSI, Switzerland

ARTICLE INFO

Article history:

Received 2 March 2015

Received in revised form 12 May 2015

Accepted 23 May 2015

Available online 27 May 2015

Editor: G.F. Giudice

ABSTRACT

We investigate the decays of the light stop in scenarios with the lightest neutralino $\tilde{\chi}_1^0$ being the lightest supersymmetric particle, including flavour-violating (FV) effects. We analyse the region where the three-body decay $\tilde{t}_1 \rightarrow Wb\tilde{\chi}_1^0$ is kinematically allowed and provide a proper description of the transition region between the three-body decay and the four-body decay $\tilde{t}_1 \rightarrow \tilde{\chi}_1^0 b f \bar{f}'$. The improved treatment has been implemented in the Fortran package SUSY-HIT and is used for the analysis of this region. A scan over the parameter range including all relevant experimental constraints reveals that the FV two-body decay into charm and $\tilde{\chi}_1^0$ can be as important as the three-, respectively, four-body decays if not dominant and therefore should be taken into account in order to complete the experimental searches for the light stop.

© 2015 The Authors. Published by Elsevier B.V. This is an open access article under the CC BY license (<http://creativecommons.org/licenses/by/4.0/>). Funded by SCOAP³.

1. Introduction

The discovery of a new scalar particle by the LHC experiments ATLAS [1] and CMS [2] has marked a milestone for particle physics. The immediate investigation of its properties allowed to identify it as the Higgs boson, i.e. the quantum fluctuation associated with the Higgs mechanism. But still, the question remains open if it is the Higgs boson of the Standard Model (SM) or of some new physics (NP) extension beyond the SM (BSM). Among the numerous NP models that are investigated, supersymmetric theories [3–17] certainly belong to the best motivated and most intensely studied BSM scenarios. Based on a symmetry between fermionic and bosonic degrees of freedom each SM particle has a supersymmetric (SUSY) counterpart. The SUSY partners of the top quark, the stops, play a special role. The large top quark mass allows for a large splitting between the two stop mass eigenstates \tilde{t}_1 and \tilde{t}_2 with interesting phenomenological consequences. Thus, while the limits on the squarks of the first two generations are pushed to higher and higher values [18,19], light stops have not been excluded yet by the experiments. Stops play an important role in the corrections to the SM-like light Higgs boson mass of the Minimal Supersymmetric Extension of the SM (MSSM) and are crucial to

shift its mass value from the tree-level upper bound given by the Z boson mass to the experimentally measured value of ~ 125 GeV. Naturalness arguments favour the stops to be light as they significantly drive the amount of fine-tuning at the electroweak scale [20]. In the MSSM with five Higgs bosons, two neutral CP-even ones, h and H , one neutral CP-odd one, A , and two charged scalars H^\pm , the maximal mixing scenario optimally reduces the amount of fine-tuning [21] while ensuring the correct mass value of h . Furthermore, light stops can help for the correct relic density through co-annihilation in scenarios with small mass differences of 15–30 GeV between the light stop and the lightest neutralino $\tilde{\chi}_1^0$ [22–27]. And last but not least, light stops are necessary for baryogenesis to generate the matter-antimatter asymmetry in the MSSM [28–40].

There exist numerous experimental analyses searching for stops in different mass windows. Light stops with masses below the kinematic threshold for the decay into a top quark and the lightest neutralino, assumed to be the lightest SUSY particle (LSP), can decay through the three-body decay $\tilde{t}_1 \rightarrow Wb\tilde{\chi}_1^0$ into the LSP, a W boson and a bottom quark b . If the \tilde{t}_1 mass lies below the three-body decay threshold, the light stop, assumed to be the next-to-lightest SUSY particle (NLSP), can decay through a FV process into the LSP and a charm quark c or an up quark u , $\tilde{t}_1 \rightarrow (u/c)\tilde{\chi}_1^0$ [41,42]. Another competing decay channel in this mass regions is the four-body decay $\tilde{t}_1 \rightarrow \tilde{\chi}_1^0 b f \bar{f}'$ [43], where f and f' stand for generic light fermions. Former bounds on the stop masses have been set by LEP [44,45] and Tevatron [46,47]. Searches based on charm tagging and monojet have been performed by ATLAS [48]

* Corresponding author.

E-mail addresses: groeber@roma3.infn.it (R. Gröber), milada.muehleitner@kit.edu (M. Mühlleitner), eva.popenda@psi.ch (E. Popenda), alexander.wlotzka@kit.edu (A. Wlotzka).

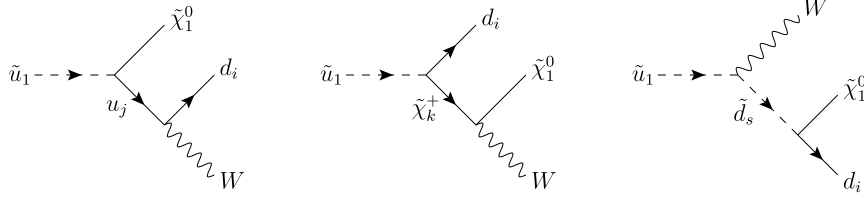


Fig. 1. Feynman diagrams of the process $\tilde{u}_1 \rightarrow W d_i \tilde{\chi}_1^0$ ($i, j = 1, 2, 3, s = 1, \dots, 6, k = 1, 2$).

and CMS [49]. More stringent bounds have been derived by ATLAS in decays into charm quarks or in compressed SUSY scenarios in [50] as well as in final states with one isolated lepton, jets and missing transverse momentum [51]. ATLAS searches in final states with two leptons have derived bounds on the stop mass under the assumption that it decays into a b -quark and an on-shell chargino, which decays via a real or virtual W boson, or that the stop decays into a top quark and the lightest neutralino [52]. The same decay modes have been taken in the analysis performed by CMS [53]. The latter analysis provides limits for various assumptions on the branching ratios, while the former analyses assume branching ratios of one in the respective final states.

In [54] we have reinterpreted the charm-tagged and monojet searches [49–51] by taking into account that the branching ratios for the FV two-body and for the four-body decay can deviate significantly from one. This leads to considerably weakened exclusion bounds. In this work we investigate the transition region at the threshold of the three-body decay $\tilde{t}_1 \rightarrow W b \tilde{\chi}_1^0$. In particular, we analyse in this threshold region the interplay between the FV two-body decay and the three-body decay above the threshold, respectively, the four-body decay just below the threshold.¹ It turns out that the two-body decay can still be significant here for certain parameter configurations and can hence be exploited to improve and/or complement analyses based on the three-body decay final states. We extend and refine former analyses [55–57] by including the recently computed SUSY-QCD corrections to the FV two-body decay [54]² and the FV tree-level couplings in the three-body decay as well as in the four-body decay where also a non-vanishing τ and bottom mass in the final state [54] are taken into account. Furthermore, the transition region between three- and four-body decays is consistently described by including a finite width in the W boson propagator, which becomes virtual below the three-body decay threshold. Finally, we check for the accordance with the LHC data on the Higgs boson search, the exclusion limits from SUSY searches as well as constraints from the relic density and B -physics and from electroweak precision measurements.

In Section 2 details on the calculation of the three- and four-body decay widths are given, followed in Section 3 by the description of the numerical analysis and the applied constraints. Our results are presented in Section 4. We conclude in Section 5.

2. Three- and four-body stop decays

We work in the framework of the MSSM with general flavour structure. Flavour-violating effects are constrained by experiment to be very small which can be naturally accounted for in the Minimal Flavour Violation (MFV) [59–63] approach, e.g., where the only sources of FV are given by the CKM matrix elements. Flavour violation is induced through renormalisation group running. Due to the large mixing in the stop sector, the lightest up-type squark \tilde{u}_1 is

then mostly stop-like. For convenience, we occasionally refer to it as the light stop \tilde{t}_1 in the following although it is understood that it has small flavour admixtures from the charm- and up-flavours. The three-body decay of \tilde{u}_1 into the lightest neutralino, a down-type fermion d_i ($i = 1, 2, 3$), where i denotes the quark flavour, and a W boson,

$$\tilde{u}_1 \rightarrow W d_i \tilde{\chi}_1^0, \quad (1)$$

proceeds via down-type squark, chargino and up-type quark exchange. The Feynman diagrams are displayed in Fig. 1. The index $s = 1, \dots, 6$ of the exchanged squark refers to one of the six squark mass eigenstates, which are not flavour eigenstates any more. In case of small FV as given in the MFV setup, the dominant final state is given by $W b \tilde{\chi}_1^0$. We have calculated the three-body decay with the general flavour structure by extending the results of [55, 57] to all flavours. The full dependence on the bottom quark mass has been taken into account, whereas the first and second generation quark masses have been set to zero. The result for the decay width has been checked against a second, independent calculation by using FeynArts/FormCalc [64–67].

In the threshold region where the three-body decay mode of the light stop into $W b \tilde{\chi}_1^0$ opens up, the off-shell effects of the W boson can be described by implementing the W boson width in the propagators of the W boson diagrams in the four-body decays

$$\tilde{u}_1 \rightarrow \tilde{\chi}_1^0 d_i f \bar{f}' . \quad (2)$$

Again in case of small FV the dominant final state is the one involving the b -quark, i.e. $d_i = b$. The W boson width in the propagators introduces a gauge dependence. The width renders the W boson mass m_W in the W boson propagators complex, whereas it is real in the corresponding Goldstone boson couplings, so that the cancellation of the gauge parameter dependence between the W boson and the associated Goldstone boson diagrams cannot take place any more. Possible solutions are given by the complex mass scheme [68], where a complex mass is introduced also in the Feynman rules, or by the overall-factor scheme [69,70], in which the whole tree-level amplitude is multiplied by

$$\prod_{W \text{ propagators}} \frac{p_W^2 - m_W^2}{p_W^2 - m_W^2 + i m_W \Gamma_W}, \quad (3)$$

where p_W denotes the W boson four momentum and Γ_W the W boson width. The product \prod accounts for the maximal number of W propagators in the amplitude. We use the overall-factor scheme to ensure a gauge independent result. The drawback of this method is that close to the threshold the non-resonant contributions are neglected. We checked, however, explicitly, that in the scenarios found in our numerical analysis below, the effect of neglecting the non-resonant contribution is less than about 2% and hence acceptable. The three-body decay and the thus calculated four-body decay widths have been implemented in the SDECAY [71,72] routine of SUSY-HIT [73], where the SUSY Les Houches Accord (SLHA) [74] format has been extended to the SLHA2 format [75], as described in Ref. [54], to account for FV.

¹ Note that we choose the parameters such that in the four-body decay only the diagrams with the intermediate W boson can become on-shell in the investigated region.

² See also [58].

In order to ensure that the three-body and the four-body decay widths match for $m_{\tilde{u}_1} - m_{\tilde{\chi}_1^0}$ mass differences above the kinematic threshold of an on-shell W boson, the W boson width must be computed in accordance with the loop order and the input values used for the computation of the four-body decay width. Thus, the tree-level W boson decay width is computed with massless first and second generation fermions, while the masses of the bottom quark and the τ lepton are kept finite.

3. Numerical setup and experimental constraints

We have performed a random scan over the parameter space of the model with the same settings as in the $U(2)$ -inspired scan of Ref. [54]. The parameters have been varied in the ranges

$$\begin{aligned} \tan \beta &\in [1, 15], \\ M_A &\in [150, 1000] \text{ GeV}, \\ M_1 &\in [75, 500] \text{ GeV}, \\ M_{\tilde{U}_3} &\in [300, 600] \text{ GeV}, \\ M_{\tilde{Q}_3} &\in [1000, 1500] \text{ GeV}, \\ A_t &\in [1000, 2000] \text{ GeV}. \end{aligned} \quad (4)$$

The remaining MSSM input parameters have been chosen as

$$\begin{aligned} M_2 &= 650 \text{ GeV}, \\ M_3 &= 1530 \text{ GeV}, \\ \mu &= 900 \text{ GeV}, \\ M_{\tilde{E}_{1,2,3}} &= M_{\tilde{L}_{1,2,3}} = 1 \text{ TeV}, \\ M_{\tilde{Q}_{1,2}} &= M_{\tilde{U}_{1,2}} = M_{\tilde{D}_{1,2,3}} = 1.5 \text{ TeV}, \\ A_U &= A_E = A_D = 0. \end{aligned} \quad (5)$$

The SM input parameters have been set to the PDG values [76]. We have applied the same constraints on the generated parameter points as in [54], but updated the branching ratio of the $B_s^0 \rightarrow \mu^+ \mu^-$ decay to the recently reported value

$$\mathcal{B}(B_s^0 \rightarrow \mu^+ \mu^-) = (2.8^{+0.7}_{-0.6}) \times 10^{-9} \quad [77]. \quad (6)$$

Additionally we have checked for the dominant restrictions due to electroweak precision observables by throwing away all points which are outside the 2σ interval around the experimental value for the ρ -parameter

$$\rho = 1.0004 \pm 0.00024 \quad [76]. \quad (7)$$

Among the parameter points fulfilling the constraints we have retained only those, for which the masses of the lightest up-type squark \tilde{u}_1 and the lightest neutralino $\tilde{\chi}_1^0$ comply with

$$m_{\tilde{u}_1} - m_{\tilde{\chi}_1^0} \in [60, 140] \text{ GeV}. \quad (8)$$

The mass window around the three- to four-body decay threshold has been chosen large enough to allow for studying all effects that emerge in the threshold region. Finally, for the parameter points above the threshold SModelS [78–80] based on the tools *Phythia* 6.4 [81], *NLL-fast* [82–88] and *PySLHA* [89], is used to ensure that all parameter points fulfil the exclusion bounds derived from direct searches by ATLAS and CMS [49–53,90]. Since the searches in the FV two-body decay channel are not covered by SModelS yet, for the parameter points below the threshold the procedure explained in [54] is used. The scenarios surviving all constraints include chargino masses around 660 GeV, slepton

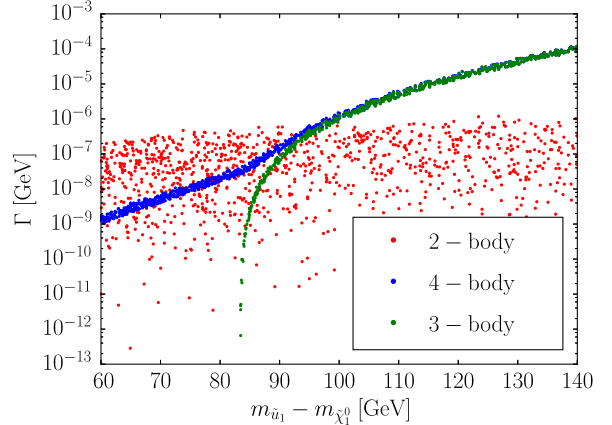


Fig. 2. Partial widths of the \tilde{u}_1 two- (red), three- (green) and four-body (blue) decays as a function of the $m_{\tilde{u}_1} - m_{\tilde{\chi}_1^0}$ mass difference. (For interpretation of the references to colours in this figure legend, the reader is referred to the web version of this article.)

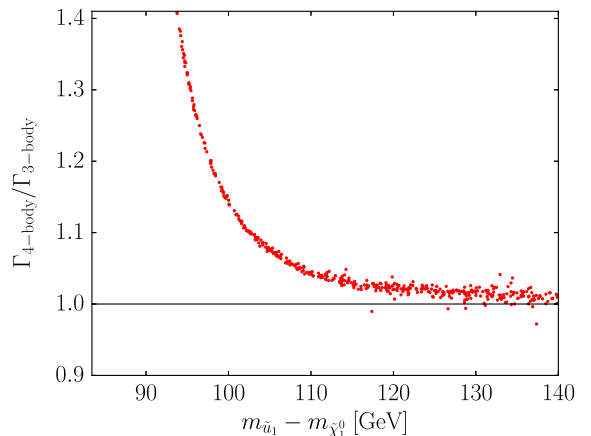


Fig. 3. Comparison of the \tilde{u}_1 four- and three-body decay widths as a function of the $m_{\tilde{u}_1} - m_{\tilde{\chi}_1^0}$ mass difference.

masses of $\mathcal{O}(1 \text{ TeV})$ and charged Higgs masses in the range ~ 400 to $\sim 1 \text{ TeV}$, so that the corresponding diagrams in the four-body decay with these particles in the intermediate propagators never go on-shell in the investigated threshold region.

4. Results

Fig. 2 shows the two-, three-, and four-body decay widths, respectively, for the parameter points of our scan which are in accordance with all applied constraints. The three-body decay, given by the green points, sets in at the threshold $m_{\tilde{u}_1} - m_{\tilde{\chi}_1^0} = m_W + m_d$. As expected, it approaches the four-body decay, illustrated by the blue points, for $m_{\tilde{u}_1} - m_{\tilde{\chi}_1^0}$ mass differences sufficiently above the threshold.³ The relative size of the four- and the three-body decay widths is displayed in Fig. 3. It shows that the finite width effects are still sizeable 20 GeV above the threshold and therefore should be taken into account, as is done by including the total width of the W boson in the four-body decay. Note, that the scattering of the points

³ Note, that we have implemented the total width of the top quark in the three-body decay and explicitly checked that the top width does not play a role in the three-body decay, also for $m_{\tilde{u}_1} - m_{\tilde{\chi}_1^0}$ mass differences as large as 140 GeV. The three-body decay with the top quark width and FV couplings has been implemented in the SUSY-HIT version that includes FV decays.

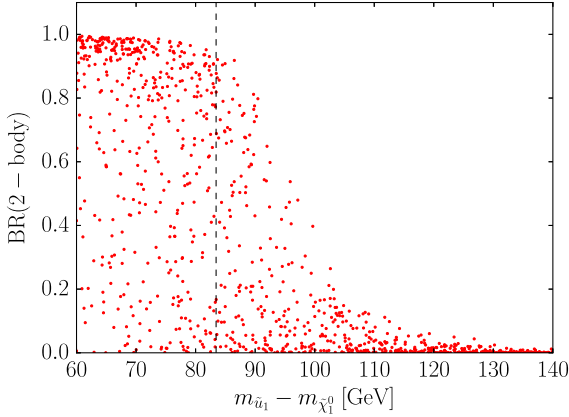


Fig. 4. Branching ratio of the \tilde{u}_1 two-body decay as a function of the $m_{\tilde{u}_1} - m_{\tilde{\chi}_1^0}$ mass difference. The dashed line marks the threshold for the three-body decay.

at the upper end of the mass difference is subject to the numerical integration precision in the four-body decay. Furthermore, the remaining off-set between the four- and three-body decay at large mass differences is due to the finite value of the W boson width.

As can be inferred from Fig. 2, the values of the two-body decay widths are equally distributed along the chosen range of the $m_{\tilde{u}_1} - m_{\tilde{\chi}_1^0}$ mass difference. While above the threshold the three-body decay dominates, close to the threshold the decay width for the two-body decay, which is shown in red, can be of similar size as the three- and four-body decay width, respectively. The branching ratio of the two-body decay is depicted in Fig. 4. With possible values as large as $\sim 40\%$ at 20 GeV above the threshold, the two-body decay clearly is competitive with the other decay modes and thereby offers new discovery perspectives for light stops in this parameter region. In this region the charm is not soft any more and charm tagging could be used efficiently, as has been shown in [91], where a search for pair produced scalar partners of charm quarks was performed. Such large two-body decay widths are achieved in scenarios with relatively large FV as is the case in the $U(2)$ -inspired scenarios investigated here. If such a set-up is realised by nature, Fig. 4 shows that it might not be possible to detect the light stop in the three- and four-body decay mode, respectively, if the masses of the light stop and the neutralino are such that they fall into the threshold regime. Hence, complementary searches in the two- and the three-, respectively, four-body decay mode are required in this case.

The two-body decay branching ratios for all scenarios of the random scan that passed the constraints are plotted in Fig. 5 in the $m_{\tilde{u}_1} - m_{\tilde{\chi}_1^0}$ mass plane. The upper and lower grey lines mark the borders of the interval defined in Eq. (8) and the colour code indicates the value of the two-body decay branching ratio. While for the low mass region the parameter space is already very constrained such that no valid parameter points with stop masses lower than 260 GeV have been found, the fade out at high values of the stop and neutralino masses in Fig. 5 is due to the limited scan range of the input parameters of the model. The plot nicely illustrates the relative importance of the two-body decay in the four- to three-body transition region and underlines once more the necessity to take this decay channel into account in order to allow for a proper analysis of the stop decays in this mass range.

5. Conclusion

In this paper we have analysed decays of the light stop including the possibility of FV and with the lightest neutralino being the LSP. We investigated in particular the mass range where the

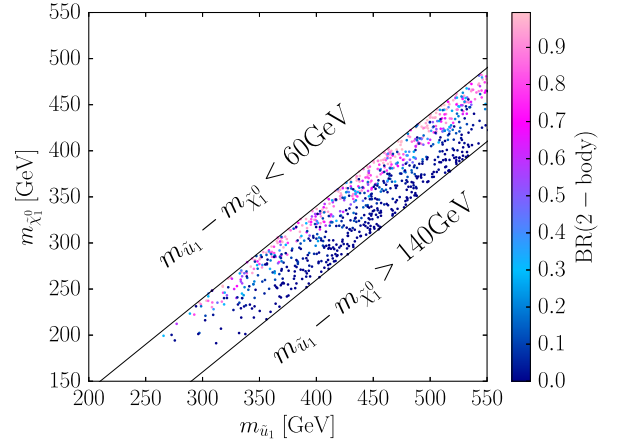


Fig. 5. Parameter points of the scan, surviving all applied constraints, in the $m_{\tilde{u}_1} - m_{\tilde{\chi}_1^0}$ plane. The colour code indicates the corresponding values of the FV two-body decay branching ratios. The upper (lower) grey line marks the lower (upper) bound of our investigated mass interval below (above) the threshold for the three-body decay. (For interpretation of the references to colours in this figure legend, the reader is referred to the web version of this article.)

three-body decay into $W b \tilde{\chi}_1^0$ is kinematically allowed. We provide a proper description of this threshold region by resorting to the four-body decay into $\tilde{\chi}_1^0 b f \bar{f}'$ where the W boson total width has been taken into account in a gauge invariant way. The resulting decay formula and the three-body decay with general flavour structure have been included in SUSY-HIT. We performed a scan over this threshold region where only the points in accordance with the constraints from the LHC Higgs and SUSY data, from the relic density and B physics measurements as well as from the electroweak precision data have been retained. The investigation of these scenarios revealed that the FV two-body decay into $c \tilde{\chi}_1^0$ can be comparable to the three-, respectively, four-body decay and even dominate for some parameter sets. In order to properly investigate this mass region, the experiments should therefore also investigate two-body decays with charm quarks in the final state, in order not to miss the light stop, which might be the first SUSY particle to be discovered at the LHC.

Acknowledgements

We are grateful to Ben Allanach and Werner Porod for discussions on the flavour implementation in their codes. M.M.M. would like to thank Filip Moortgat and Michael Spira for discussions on stop decays. A.W. acknowledges support by the “Karlsruhe School of Elementary Particle and Astroparticle Physics: Science and Technology (KSETA)”.

Appendix A. Three-body decay width

In this appendix we give the analytic formula for the decay width of the process $\tilde{u}_1 \rightarrow W d_i \tilde{\chi}_1^0$. We first define the couplings relevant for the decay width. The coupling of an up-type and down-type squark to the W boson, with the corresponding part of the Lagrangian given by $\mathcal{L} = g_{W \tilde{u}_i \tilde{d}_t} \tilde{d}_t^\dagger \tilde{u}_i W^-$, is defined as

$$g_{W \tilde{u}_i \tilde{d}_t} = -\frac{g_2}{\sqrt{2}} \sum_{i,j=1}^3 W_{si}^{\tilde{u}*} V_{ij}^{CKM*} W_{tj}^{\tilde{d}}, \quad (\text{A.1})$$

where V^{CKM} denotes the CKM matrix, $W^{\tilde{u}}$ and $W^{\tilde{d}}$ the squark mixing matrices in the SCKM basis as defined in the SLHA2 convention [75] and g_2 the $SU(2)_L$ coupling constant. The squark-

quark–neutralino couplings to up-type quarks and squarks, with $\mathcal{L} = \tilde{u}_i(g_{\chi u_i \tilde{u}_s}^R P_L + g_{\chi u_i \tilde{u}_s}^L P_R)\tilde{u}_s \tilde{\chi}_1^0$, are defined as

$$\begin{aligned} g_{\chi u_i \tilde{u}_s}^L &= -\sqrt{2} \left(\frac{1}{2} g_2 Z_{12} + \frac{1}{6} g_1 Z_{11} \right) W_{si}^{\tilde{u}*} \\ &\quad - \frac{g_2}{\sqrt{2}m_W \sin \beta} m_{u_i} Z_{14} W_{si+3}^{\tilde{u}*} \end{aligned} \quad (\text{A.2})$$

$$\begin{aligned} g_{\chi u_i \tilde{u}_s}^R &= \frac{2}{3} \sqrt{2} g_1 Z_{11}^* W_{si+3}^{\tilde{u}*} \\ &\quad - \frac{g_2}{\sqrt{2}m_W \sin \beta} m_{u_i} Z_{14}^* W_{si}^{\tilde{u}*}, \end{aligned} \quad (\text{A.3})$$

and the ones to down-type squarks and quarks, with $\mathcal{L} = \tilde{d}_i(g_{\chi d_i \tilde{d}_s}^R P_L + g_{\chi d_i \tilde{d}_s}^L P_R)\tilde{d}_s \tilde{\chi}_1^0$, as

$$\begin{aligned} g_{\chi d_i \tilde{d}_s}^L &= \sqrt{2} \left(\frac{1}{2} g_2 Z_{12} - \frac{1}{6} g_1 Z_{11} \right) W_{si}^{\tilde{d}*} \\ &\quad - \frac{g_2}{\sqrt{2}m_W \cos \beta} m_{d_i} Z_{13} W_{si+3}^{\tilde{d}*} \end{aligned} \quad (\text{A.4})$$

$$\begin{aligned} g_{\chi d_i \tilde{d}_s}^R &= -\frac{1}{3} \sqrt{2} g_1 Z_{11}^* W_{si+3}^{\tilde{d}*} \\ &\quad - \frac{g_2}{\sqrt{2}m_W \cos \beta} m_{d_i} Z_{13}^* W_{si}^{\tilde{d}*}. \end{aligned} \quad (\text{A.5})$$

Here, the W boson mass is denoted by m_W , g_1 is the $U(1)_Y$ coupling constant and Z the neutralino mixing matrix as defined according to the conventions in Ref. [75]. The angle β is determined through $\tan \beta = v_u/v_d$ where $v_{u,d}$ denote the vacuum expectation values of $H_{u,d}$, respectively. The squark–quark–chargino couplings, with $\mathcal{L} = \tilde{d}_i \left(g_{\chi_l^+ d_i \tilde{u}_s}^L P_R + g_{\chi_l^+ d_i \tilde{u}_s}^R P_L \right) \tilde{u}_s \tilde{\chi}_l^-$, are given by

$$\begin{aligned} g_{\chi_l^+ d_i \tilde{u}_s}^L &= \frac{g_2}{\sqrt{2}m_W \sin \beta} V_{l2} \sum_{j=1}^3 m_{u_j} V_{ji}^{CKM*} W_{sj+3}^{\tilde{u}*} \\ &\quad - g_2 V_{l1} \sum_{j=1}^3 W_{sj}^{\tilde{u}*} V_{ji}^{CKM*} \end{aligned} \quad (\text{A.6})$$

$$g_{\chi_l^+ d_i \tilde{u}_s}^R = \frac{g_2}{\sqrt{2}m_W \cos \beta} U_{k2}^* m_{d_i} \sum_{j=1}^3 W_{sj}^{\tilde{u}*} V_{ji}^{CKM*}, \quad (\text{A.7})$$

with U and V denoting the chargino mixing matrices as defined in [74]. The chargino–neutralino– W boson coupling given by $\mathcal{L} = \tilde{\chi}_1^-(g_{\chi_k^+ \chi_1}^L P_R + g_{\chi_k^+ \chi_1}^R P_L)\tilde{\chi}_1^0 W^-$, is defined as

$$g_{\chi_k^+ \chi_1}^L = g_2 \left(Z_{12} V_{k1}^* - \frac{1}{\sqrt{2}} Z_{14} V_{k2}^* \right) \quad (\text{A.8})$$

$$g_{\chi_k^+ \chi_1}^R = g_2 \left(Z_{12}^* U_{k1} + \frac{1}{\sqrt{2}} Z_{13}^* U_{k2} \right). \quad (\text{A.9})$$

Furthermore we introduce

$$\mu_\chi = \frac{m_\chi^2}{m_{\tilde{u}_1}^2}. \quad (\text{A.10})$$

Note that we will drop the indices for $\tilde{\chi}_1^0$ and denote the corresponding μ with μ_χ . By d_i we denote the final state down-type fermion with flavour index i . In SUSY-HIT we have set the masses of the first and second generation quarks to zero, corresponding to $\mu_{d_{1,2}} = 0$ and $\mu_{u_{1,2}} = 0$. The differential decay width can then be written as

$$\begin{aligned} d\Gamma &= \frac{m_{\tilde{u}_1}}{32(2\pi)^3} \operatorname{Re} \left[|\mathcal{M}_{\tilde{d}}|^2 + |\mathcal{M}_{\chi^+}|^2 + |\mathcal{M}_u|^2 \right. \\ &\quad \left. + 2\mathcal{M}_{\tilde{d}} \mathcal{M}_{\chi^+}^* + 2\mathcal{M}_{\tilde{d}} \mathcal{M}_u^* + 2\mathcal{M}_{\chi^+} \mathcal{M}_u^* \right] dx_1 dx_2 \end{aligned} \quad (\text{A.11})$$

and needs to be integrated over the reduced energies of the final state particles $x_1 = 2(p_{\tilde{u}_1} \cdot p_{d_i})/m_{\tilde{u}_1}^2$ and $x_2 = 2(p_{\tilde{u}_1} \cdot p_\chi)/m_{\tilde{u}_1}^2$ with p_X denoting the four-momentum of particle X . The integration limits for the reduced energy x_1 are given by

$$(x_1)_{\min} = 2\sqrt{\mu_{d_i}} \quad (\text{A.12})$$

$$(x_1)_{\max} = 1 + \mu_{d_i} - \frac{(m_W + m_\chi)^2}{m_{\tilde{u}_1}^2}. \quad (\text{A.13})$$

For a given value of x_1 the range of x_2 is determined by

$$\begin{aligned} (x_2)_{\min} &= 1 + \mu_\chi - \frac{(E_W + E_{d_i})^2}{m_{\tilde{u}_1}^2} \\ &\quad + \frac{\left(\sqrt{E_W^2 - m_W^2} - \sqrt{E_{d_i}^2 - m_{d_i}^2} \right)^2}{m_{\tilde{u}_1}^2} \end{aligned} \quad (\text{A.14})$$

$$\begin{aligned} (x_2)_{\max} &= 1 + \mu_\chi - \frac{(E_W + E_{d_i})^2}{m_{\tilde{u}_1}^2} \\ &\quad + \frac{\left(\sqrt{E_W^2 - m_W^2} + \sqrt{E_{d_i}^2 - m_{d_i}^2} \right)^2}{m_{\tilde{u}_1}^2}. \end{aligned} \quad (\text{A.15})$$

Here E_W and E_{d_i} are the energies of the W boson and the down-type quark d_i evaluated in the rest frame of the incoming stop and neutralino,

$$E_W = \frac{m_{\tilde{u}_1}^2 - m_{\tilde{u}_1}^2 x_1 + m_{d_i}^2 - m_\chi^2 + m_W^2}{2\sqrt{m_{\tilde{u}_1}^2 - m_{\tilde{u}_1}^2 x_1 + m_{d_i}^2}} \quad (\text{A.16})$$

$$E_{d_i} = \frac{m_{\tilde{u}_1}^2 x_1 - 2m_{d_i}^2}{2\sqrt{m_{\tilde{u}_1}^2 - m_{\tilde{u}_1}^2 x_1 + m_{d_i}^2}}. \quad (\text{A.17})$$

The individual contributions to the differential decay width in Eq. (A.11) read

$$\begin{aligned} |\mathcal{M}_{\tilde{d}}|^2 &= 8 \sum_{s,t=1}^6 g_{W \tilde{u}_1 \tilde{d}_s} g_{W \tilde{u}_1 \tilde{d}_t}^* \left\{ \left(g_{\chi d_i \tilde{d}_s}^L g_{\chi d_i \tilde{d}_t}^{L*} + g_{\chi d_i \tilde{d}_s}^R g_{\chi d_i \tilde{d}_t}^{R*} \right) \right. \\ &\quad \times \frac{y_1 [\mu_W^{-1} (y_2 + y_3)^2 - \mu_\chi - \mu_{d_i} - 2y_1]}{(1 - x_3 + \mu_W - \mu_{\tilde{d}_s})(1 - x_3 + \mu_W - \mu_{\tilde{d}_t})} \\ &\quad + \left. \left(g_{\chi d_i \tilde{d}_s}^L g_{\chi d_i \tilde{d}_t}^{R*} + g_{\chi d_i \tilde{d}_s}^R g_{\chi d_i \tilde{d}_t}^{L*} \right) \sqrt{\mu_{d_i} \mu_\chi} \right. \\ &\quad \times \frac{2y_1 + \mu_\chi + \mu_{d_i} - \mu_W^{-1} (y_2 + y_3)^2}{(1 - x_3 + \mu_W - \mu_{\tilde{d}_s})(1 - x_3 + \mu_W - \mu_{\tilde{d}_t})} \left. \right\} \quad (\text{A.18}) \end{aligned}$$

$$\begin{aligned} |\mathcal{M}_u|^2 &= \sum_{j,k=1}^3 \frac{g_2^2 V_{kn}^{CKM} V_{jn}^{CKM*}}{2(1 - x_2 + \mu_\chi - \tilde{\mu}_{u_k})(1 - x_2 + \mu_\chi - \tilde{\mu}_{u_j})} \\ &\quad \times \left\{ -2 \left(\sqrt{\mu_{u_k}} g_{\chi u_k \tilde{u}_1}^R g_{\chi u_j \tilde{u}_1}^{L*} + (k \leftrightarrow j) \right) \right. \\ &\quad \times \sqrt{\mu_\chi} \left(\mu_{d_i} + 3y_2 + 2y_2^2 \mu_W^{-1} \right) \\ &\quad \left. + 2g_{\chi u_k \tilde{u}_1}^R g_{\chi u_j \tilde{u}_1}^{R*} \sqrt{\mu_{u_k} \mu_{u_j}} \left(y_1 + 2y_2 y_3 \mu_W^{-1} \right) \right\} \end{aligned}$$

$$+ 2g_{\chi u_k \tilde{u}_1}^L g_{\chi u_j \tilde{u}_1}^{L*} (y_1(\mu_{d_i} - \mu_W + 4y_2) + 2y_3\mu_{d_i} \\ + 4y_2y_3 + \mu_W^{-1}(4y_1y_2^2 - 2y_2y_3\mu_{d_i})) \Big\}, \quad (\text{A.19})$$

with $\tilde{\mu}_{u_3} = \mu_{u_3} + i\sqrt{\mu_{u_3}}\Gamma_t/m_{\tilde{u}_1}$ and Γ_t denoting the top width. For $i=1,2$ the $\tilde{\mu}_{u_i}$ are equal to μ_{u_i} .

$$|\mathcal{M}_{\chi^+}|^2 = \sum_{k,l=1}^2 \frac{2}{(1-x_1-\mu_{\chi_k^+})(1-x_1-\mu_{\chi_l^+})} \\ \times \left\{ \left(g_{\chi_k^+ d_i \tilde{u}_1}^L g_{\chi_l^+ d_i \tilde{u}_1}^{L*} g_{\chi_k^+ \chi_1}^L g_{\chi_l^+ \chi_1}^{L*} + (R \leftrightarrow L) \right) \right. \\ \times \left[4y_3(y_1+y_2+\mu_W^{-1}y_1y_3) + y_1(\mu_\chi - \mu_W) \right. \\ \left. + 2\mu_\chi y_2(1-\mu_W^{-1}y_3) \right] \\ + \left(g_{\chi_k^+ d_i \tilde{u}_1}^L g_{\chi_l^+ d_i \tilde{u}_1}^{L*} g_{\chi_k^+ \chi_1}^R g_{\chi_l^+ \chi_1}^{R*} + (R \leftrightarrow L) \right) \\ \times \sqrt{\mu_{\chi_k^+}\mu_{\chi_l^+}}(y_1+2\mu_W^{-1}y_2y_3) \\ - \left[\left(g_{\chi_k^+ d_i \tilde{u}_1}^L g_{\chi_l^+ d_i \tilde{u}_1}^{L*} g_{\chi_k^+ \chi_1}^R g_{\chi_l^+ \chi_1}^{L*} + (R \leftrightarrow L) \right) \right. \\ \times \sqrt{\mu_{\chi_k^+}} + (k \leftrightarrow l) \left. \right] 3\sqrt{\mu_\chi}(y_1+y_2) \\ - \left[\left(g_{\chi_k^+ d_i \tilde{u}_1}^L g_{\chi_l^+ d_i \tilde{u}_1}^{R*} g_{\chi_k^+ \chi_1}^R g_{\chi_l^+ \chi_1}^{R*} + (R \leftrightarrow L) \right) \right. \\ \times \sqrt{\mu_{d_i}\mu_{\chi_k^+}} + (k \leftrightarrow l) \left. \right] (\mu_\chi + 2y_3^2\mu_W^{-1} + 3y_3) \\ + \left(g_{\chi_k^+ d_i \tilde{u}_1}^L g_{\chi_l^+ d_i \tilde{u}_1}^{R*} g_{\chi_k^+ \chi_1}^L g_{\chi_l^+ \chi_1}^{L*} + (R \leftrightarrow L) \right) \\ \times 3\sqrt{\mu_{d_i}\mu_\chi\mu_{\chi_l^+}\mu_{\chi_k^+}} \\ + \left(g_{\chi_k^+ d_i \tilde{u}_1}^L g_{\chi_l^+ d_i \tilde{u}_1}^{R*} g_{\chi_k^+ \chi_1}^L g_{\chi_l^+ \chi_1}^{R*} + (R \leftrightarrow L) \right) \\ \times 3\sqrt{\mu_{d_i}\mu_\chi}(\mu_W + \mu_\chi + 2y_3) \Big\}. \quad (\text{A.20})$$

The interference terms read

$$\mathcal{M}_{\tilde{d}} \mathcal{M}_{\chi^+}^* = \sum_{s=1}^6 \sum_{l=1}^2 \frac{-4g_{W \tilde{u}_1 \tilde{d}_s}}{(1-x_3+\mu_W-\mu_{\tilde{d}_s})(1-x_1-\mu_{\chi_l^+})} \\ \times \left\{ \left(g_{\chi_l^+ d_i \tilde{u}_1}^L g_{\chi_l^+ \chi_1}^{R*} g_{\chi d_i \tilde{d}_s}^L + (R \leftrightarrow L) \right) \right. \\ \times \sqrt{\mu_\chi\mu_{\chi_l^+}}(y_1-y_2\mu_W^{-1}(y_2+y_3)+\mu_{d_i}) \\ + \left(g_{\chi_l^+ d_i \tilde{u}_1}^L g_{\chi_l^+ \chi_1}^{L*} g_{\chi d_i \tilde{d}_s}^L + (R \leftrightarrow L) \right) \\ \times \left[(y_2+y_3)(\mu_\chi y_2 - 2y_1y_3)\mu_W^{-1} + y_1(2y_1+y_2 \right. \\ \left. - y_3 + \mu_\chi) + \mu_\chi y_2 - \mu_{d_i}(\mu_\chi + y_3) \right] \\ + (\mu_W^{-1}y_3(y_2+y_3) - \mu_\chi - y_1) \\ \times \left[\sqrt{\mu_{d_i}\mu_\chi} \left(g_{\chi_l^+ d_i \tilde{u}_1}^{R*} g_{\chi_l^+ \chi_1}^L g_{\chi d_i \tilde{d}_s}^L + (R \leftrightarrow L) \right) \right. \\ \left. + \sqrt{\mu_{d_i}\mu_{\chi_l^+}} \left(g_{\chi_l^+ d_i \tilde{u}_1}^{R*} g_{\chi_l^+ \chi_1}^L g_{\chi d_i \tilde{d}_s}^L + (R \leftrightarrow L) \right) \right] \Big\}$$

$$\mathcal{M}_{\tilde{d}} \mathcal{M}_u^* = \sum_{s=1}^6 \sum_{j=1}^3 \frac{-2\sqrt{2}g_2 g_{W \tilde{u}_1 \tilde{d}_s}}{(1-x_3+\mu_\chi-\mu_{\tilde{d}_s})(1-x_2+\mu_\chi-\tilde{\mu}_{u_j})} \\ \times V_{jn}^{CKM*} \left\{ \sqrt{\mu_{u_j}\mu_\chi} g_{\chi u_j \tilde{u}_1}^{R*} g_{\chi d_i \tilde{d}_s}^L \right. \\ \times \left[y_1 + \mu_{d_i} - y_2\mu_W^{-1}(y_2+y_3) \right] \\ + g_{\chi u_j \tilde{u}_1}^{L*} g_{\chi d_i \tilde{d}_s}^L \left[y_1 y_2 \left(1 + 2\mu_W^{-1}(y_2+y_3) \right) \right. \\ + \mu_\chi y_2 - y_1 y_3 - 2y_1^2 - y_1 \mu_{d_i} \\ + \mu_{d_i}(\mu_\chi - y_3) + \mu_W^{-1}\mu_{d_i}(-y_2y_3 - y_3^2) \\ + g_{\chi u_j \tilde{u}_1}^{R*} g_{\chi d_i \tilde{d}_s}^R \sqrt{\mu_{d_i}\mu_{u_j}} \left[-y_1 - \mu_\chi \right. \\ \left. + \mu_W^{-1}y_3(y_2+y_3) \right] + g_{\chi u_j \tilde{u}_1}^{L*} g_{\chi d_i \tilde{d}_s}^R \sqrt{\mu_{d_i}\mu_\chi} \\ \times \left[y_1 + \mu_{d_i} - \mu_W^{-1}y_2(y_2+y_3) \right] \Big\} \quad (\text{A.22})$$

$$\mathcal{M}_{\chi^+} \mathcal{M}_u^* = \sum_{k=1}^2 \sum_{j=1}^3 \frac{g_2}{\sqrt{2}(1-x_1-\mu_{\chi_k^+})(1-x_2+\mu_\chi-\tilde{\mu}_{u_j})} \\ \times V_{jn}^{CKM*} \left\{ g_{\chi_k^+ d_i \tilde{u}_1}^L g_{\chi_k^+ \chi_1}^R g_{\chi u_j \tilde{u}_1}^{L*} \sqrt{\mu_\chi\mu_{\chi_k^+}} \right. \\ \times (-6y_2 - 4\mu_W^{-1}y_2^2 - 2\mu_{d_i}) \\ + 2g_{\chi_k^+ d_i \tilde{u}_1}^L g_{\chi_k^+ \chi_1}^L g_{\chi u_j \tilde{u}_1}^{L*} \\ \times \left[y_1(2y_3 + 2y_2 + 4y_1 - \mu_W) + y_2(4y_3 + \mu_\chi) \right. \\ \left. - 2y_2(2y_1y_3 - \mu_\chi y_2)\mu_W^{-1} + 2\mu_{d_i}\mu_W^{-1}y_3^2 \right. \\ \left. - \mu_{d_i}\mu_\chi + \mu_{d_i}y_3 \right] \\ - 6\sqrt{\mu_{u_j}\mu_\chi} g_{\chi_k^+ d_i \tilde{u}_1}^L g_{\chi_k^+ \chi_1}^L g_{\chi u_j \tilde{u}_1}^{R*} (y_1+y_2) \\ + \sqrt{\mu_{u_j}\mu_{\chi_k^+}} g_{\chi_k^+ d_i \tilde{u}_1}^L g_{\chi_k^+ \chi_1}^R g_{\chi u_j \tilde{u}_1}^{R*} \\ \times (2y_1 + 4\mu_W^{-1}y_2y_3) \\ + g_{\chi_k^+ d_i \tilde{u}_1}^R g_{\chi_k^+ \chi_1}^R g_{\chi u_j \tilde{u}_1}^{R*} \sqrt{\mu_{d_i}\mu_{u_j}} \\ \times (-6y_3 - 4y_3^2\mu_W^{-1} - 2\mu_\chi) \\ + 6g_{\chi_k^+ d_i \tilde{u}_1}^R g_{\chi_k^+ \chi_1}^L g_{\chi u_j \tilde{u}_1}^{R*} \sqrt{\mu_{d_i}\mu_{u_j}\mu_\chi\mu_{\chi_k^+}} \\ - 6g_{\chi_k^+ d_i \tilde{u}_1}^R g_{\chi_k^+ \chi_1}^L g_{\chi u_j \tilde{u}_1}^{L*} \sqrt{\mu_{d_i}\mu_{\chi_k^+}} (y_1+y_3) \\ + g_{\chi_k^+ d_i \tilde{u}_1}^R g_{\chi_k^+ \chi_1}^R g_{\chi u_j \tilde{u}_1}^{L*} \sqrt{\mu_{d_i}\mu_\chi} \left[6\mu_W + 6y_3 \right. \\ \left. + 6y_2 + 2y_1 + 4\mu_W^{-1}y_2y_3 \right] \Big\}. \quad (\text{A.23})$$

In Eqs. (A.18)–(A.23) we have used

$$x_3 = 2 - x_1 - x_2 \quad (\text{A.24})$$

$$y_1 = \frac{1}{2}(1 + \mu_W - \mu_\chi - \mu_{d_i} - x_3) \quad (\text{A.25})$$

$$y_2 = \frac{1}{2}(1 - \mu_W + \mu_\chi - \mu_{d_i} - x_2) \quad (\text{A.26})$$

$$y_3 = \frac{1}{2}(1 - \mu_W - \mu_\chi + \mu_{d_i} - x_1). \quad (\text{A.27})$$

The notation ($R \leftrightarrow L$) means that the respective term is obtained from the previous one by replacing $R \leftrightarrow L$ in the couplings, whereas ($k \leftrightarrow l$) and ($k \leftrightarrow j$) means that the term is obtained by interchanging indices k and l or k and j , respectively.

References

- [1] ATLAS Collaboration, G. Aad, et al., Observation of a new particle in the search for the Standard Model Higgs boson with the ATLAS detector at the LHC, *Phys. Lett. B* 716 (2012) 1–29, arXiv:1207.7214 [hep-ex].
- [2] CMS Collaboration, S. Chatrchyan, et al., Observation of a new boson at a mass of 125 GeV with the CMS experiment at the LHC, *Phys. Lett. B* 716 (2012) 30–61, arXiv:1207.7235 [hep-ex].
- [3] D. Volkov, V. Akulov, Is the neutrino a Goldstone particle?, *Phys. Lett. B* 46 (1973) 109–110.
- [4] J. Wess, B. Zumino, Supergauge transformations in four-dimensions, *Nucl. Phys. B* 70 (1974) 39–50.
- [5] P. Fayet, Supersymmetry and weak, electromagnetic and strong interactions, *Phys. Lett. B* 64 (1976) 159.
- [6] P. Fayet, Spontaneously broken supersymmetric theories of weak, electromagnetic and strong interactions, *Phys. Lett. B* 69 (1977) 489.
- [7] P. Fayet, Relations between the masses of the superpartners of leptons and quarks, the goldstino couplings and the neutral currents, *Phys. Lett. B* 84 (1979) 416.
- [8] G.R. Farrar, P. Fayet, Phenomenology of the production, decay, and detection of new hadronic states associated with supersymmetry, *Phys. Lett. B* 76 (1978) 575–579.
- [9] S. Dimopoulos, H. Georgi, Softly broken supersymmetry and SU(5), *Nucl. Phys. B* 193 (1981) 150.
- [10] N. Sakai, Naturalness in supersymmetric guts, *Z. Phys. C* 11 (1981) 153.
- [11] E. Witten, Dynamical breaking of supersymmetry, *Nucl. Phys. B* 188 (1981) 513.
- [12] H.P. Nilles, Supersymmetry, supergravity and particle physics, *Phys. Rep.* 110 (1984) 1–162.
- [13] H.E. Haber, G.L. Kane, The search for supersymmetry: probing physics beyond the standard model, *Phys. Rep.* 117 (1985) 75–263.
- [14] M. Sohnius, Introducing supersymmetry, *Phys. Rep.* 128 (1985) 39–204.
- [15] J. Gunion, H.E. Haber, Higgs bosons in supersymmetric models. 1., *Nucl. Phys. B* 272 (1986) 1.
- [16] J. Gunion, H.E. Haber, Higgs bosons in supersymmetric models. 2. Implications for phenomenology, *Nucl. Phys. B* 278 (1986) 449.
- [17] A. Lahanas, D.V. Nanopoulos, The road to no scale supergravity, *Phys. Rep.* 145 (1987) 1.
- [18] ATLAS Collaboration, G. Aad, et al., Search for squarks and gluinos with the ATLAS detector in final states with jets and missing transverse momentum using $\sqrt{s} = 8$ TeV proton–proton collision data, *J. High Energy Phys.* 1409 (2014) 176, arXiv:1405.7875 [hep-ex].
- [19] CMS Collaboration, Search for supersymmetry in hadronic final states using MT2 with the CMS detector at $\sqrt{s} = 8$ TeV, 2013, CMS-PAS-SUS-13-019.
- [20] S. Dimopoulos, G. Giudice, Naturalness constraints in supersymmetric theories with nonuniversal soft terms, *Phys. Lett. B* 357 (1995) 573–578, arXiv:hep-ph/9507282.
- [21] C. Wymant, Optimising stop naturalness, *Phys. Rev. D* 86 (2012) 115023, arXiv:1208.1737 [hep-ph].
- [22] C. Boehm, A. Djouadi, M. Drees, Light scalar top quarks and supersymmetric dark matter, *Phys. Rev. D* 62 (2000) 035012, arXiv:hep-ph/9911496.
- [23] J.R. Ellis, K.A. Olive, Y. Santoso, Calculations of neutralino stop coannihilation in the CMSSM, *Astropart. Phys.* 18 (2003) 395–432, arXiv:hep-ph/0112113.
- [24] C. Balazs, M.S. Carena, C. Wagner, Dark matter, light stops and electroweak baryogenesis, *Phys. Rev. D* 70 (2004) 015007, arXiv:hep-ph/0403224.
- [25] C. Balazs, M.S. Carena, A. Menon, D. Morrissey, C. Wagner, The supersymmetric origin of matter, *Phys. Rev. D* 71 (2005) 075002, arXiv:hep-ph/0412264.
- [26] A. De Simone, G.F. Giudice, A. Strumia, Benchmarks for dark matter searches at the LHC, *J. High Energy Phys.* 1406 (2014) 081, arXiv:1402.6287 [hep-ph].
- [27] J. Ellis, K.A. Olive, J. Zheng, The extent of the stop coannihilation strip, *Eur. Phys. J. C* 74 (2014) 2947, arXiv:1404.5571 [hep-ph].
- [28] M.S. Carena, M. Quiros, C. Wagner, Opening the window for electroweak baryogenesis, *Phys. Lett. B* 380 (1996) 81–91, arXiv:hep-ph/9603420.
- [29] M.S. Carena, M. Quiros, C. Wagner, Electroweak baryogenesis and Higgs and stop searches at LEP and the Tevatron, *Nucl. Phys. B* 524 (1998) 3–22, arXiv:hep-ph/9710401.
- [30] B. de Carlos, J. Espinosa, The Baryogenesis window in the MSSM, *Nucl. Phys. B* 503 (1997) 24–54, arXiv:hep-ph/9703212.
- [31] P. Huet, A.E. Nelson, Electroweak baryogenesis in supersymmetric models, *Phys. Rev. D* 53 (1996) 4578–4597, arXiv:hep-ph/9506477.
- [32] D. Delepine, J. Gerard, R. Gonzalez Felipe, J. Weyers, A light stop and electroweak baryogenesis, *Phys. Lett. B* 386 (1996) 183–188, arXiv:hep-ph/9604440.
- [33] M. Losada, The two loop finite temperature effective potential of the MSSM and baryogenesis, *Nucl. Phys. B* 537 (1999) 3–31, arXiv:hep-ph/9806519.
- [34] M. Losada, Mixing effects in the finite temperature effective potential of the MSSM with a light stop, *Nucl. Phys. B* 569 (2000) 125–157, arXiv:hep-ph/9905441.
- [35] V. Cirigliano, S. Profumo, M.J. Ramsey-Musolf, Baryogenesis, electric dipole moments and dark matter in the MSSM, *J. High Energy Phys.* 0607 (2006) 002, arXiv:hep-ph/0603246.
- [36] Y. Li, S. Profumo, M. Ramsey-Musolf, Bino-driven electroweak baryogenesis with highly suppressed electric dipole moments, *Phys. Lett. B* 673 (2009) 95–100, arXiv:0811.1987 [hep-ph].
- [37] V. Cirigliano, Y. Li, S. Profumo, M.J. Ramsey-Musolf, MSSM baryogenesis and electric dipole moments: an update on the phenomenology, *J. High Energy Phys.* 1001 (2010) 002, arXiv:0910.4589 [hep-ph].
- [38] M. Carena, G. Nardini, M. Quiros, C.E. Wagner, The effective theory of the light stop scenario, *J. High Energy Phys.* 0810 (2008) 062, arXiv:0806.4297 [hep-ph].
- [39] M. Carena, G. Nardini, M. Quiros, C. Wagner, The baryogenesis window in the MSSM, *Nucl. Phys. B* 812 (2009) 243–263, arXiv:0809.3760 [hep-ph].
- [40] M. Laine, G. Nardini, K. Rummukainen, Lattice study of an electroweak phase transition at $m_h \sim 126$ GeV, *J. Cosmol. Astropart. Phys.* 1301 (2013) 011, arXiv:1211.7344 [hep-ph].
- [41] K.-i. Hikasa, M. Kobayashi, Light scalar top at e^+e^- colliders, *Phys. Rev. D* 36 (1987) 724.
- [42] M. Mühlleitner, E. Popenda, Light stop decay in the MSSM with minimal flavour violation, *J. High Energy Phys.* 1104 (2011) 095, arXiv:1102.5712 [hep-ph].
- [43] C. Boehm, A. Djouadi, Y. Mambrini, Decays of the lightest top squark, *Phys. Rev. D* 61 (2000) 095006, arXiv:hep-ph/9907428.
- [44] OPAL Collaboration, G. Abbiendi, et al., Search for scalar top and scalar bottom quarks at $S^{1/2} = 189$ GeV at LEP, *Phys. Lett. B* 456 (1999) 95–106, arXiv:hep-ex/9903070.
- [45] OPAL Collaboration, G. Abbiendi, et al., Search for scalar top and scalar bottom quarks at LEP, *Phys. Lett. B* 545 (2002) 272–284, arXiv:hep-ex/0209026.
- [46] D0 Collaboration, V. Abazov, et al., Search for scalar top quarks in the acoplanar charm jets and missing transverse energy final state in $p\bar{p}$ collisions at $\sqrt{s} = 1.96$ TeV, *Phys. Lett. B* 665 (2008) 1–8, arXiv:0803.2263 [hep-ex].
- [47] CDF Collaboration, T. Altonen, et al., Search for scalar top quark production in $p\bar{p}$ collisions at $\sqrt{s} = 1.96$ TeV, *J. High Energy Phys.* 1210 (2012) 158, arXiv:1203.4171 [hep-ex].
- [48] ATLAS Collaboration, Search for pair-produced top squarks decaying into a charm quark and the lightest neutralinos with 20.3 fb^{-1} of pp collisions at $\sqrt{s} = 8$ TeV with the ATLAS detector at the LHC, 2013, ATLAS-CONF-2013-068.
- [49] CMS Collaboration, Search for top squarks decaying to a charm quark and a neutralino in events with a jet and missing transverse momentum, 2013, CMS-PAS-SUS-13-009.
- [50] ATLAS Collaboration, G. Aad, et al., Search for pair-produced third-generation squarks decaying via charm quarks or in compressed supersymmetric scenarios in pp collisions at $\sqrt{s} = 8$ TeV with the ATLAS detector, *Phys. Rev. D* 90 (2014) 052008, arXiv:1407.0608 [hep-ex].
- [51] ATLAS Collaboration, G. Aad, et al., Search for top squark pair production in final states with one isolated lepton, jets, and missing transverse momentum in $\sqrt{s} = 8$ TeV pp collisions with the ATLAS detector, *J. High Energy Phys.* 1411 (2014) 118, arXiv:1407.0583 [hep-ex].
- [52] ATLAS Collaboration, G. Aad, et al., Search for direct top-squark pair production in final states with two leptons in pp collisions at $\sqrt{s} = 8$ TeV with the ATLAS detector, *J. High Energy Phys.* 1406 (2014) 124, arXiv:1403.4853 [hep-ex].
- [53] CMS Collaboration, S. Chatrchyan, et al., Search for top-squark pair production in the single-lepton final state in pp collisions at $\sqrt{s} = 8$ TeV, *Eur. Phys. J. C* 73 (12) (2013) 2677, arXiv:1308.1586 [hep-ex].
- [54] R. Grober, M. Mühlleitner, E. Popenda, A. Wlotzka, Light stop decays: implications for LHC searches, arXiv:1408.4662 [hep-ph].
- [55] W. Porod, T. Wohrmann, Higher order top squark decays, *Phys. Rev. D* 55 (1997) 2907–2917, arXiv:hep-ph/9608472.
- [56] W. Porod, More on higher order decays of the lighter top squark, *Phys. Rev. D* 59 (1999) 095009, arXiv:hep-ph/9812230.
- [57] A. Djouadi, Y. Mambrini, Three body decays of top and bottom squarks, *Phys. Rev. D* 63 (2001) 115005, arXiv:hep-ph/0011364.

- [58] J. Aebischer, A. Crivellin, C. Greub, One-loop SQCD corrections to the decay of top squarks to charm and neutralino in the generic MSSM, Phys. Rev. D 91 (3) (2015) 035010, arXiv:1410.8459 [hep-ph].
- [59] R.S. Chivukula, H. Georgi, L. Randall, A composite technicolor standard model of quarks, Nucl. Phys. B 292 (1987) 93–108.
- [60] L. Hall, L. Randall, Weak scale effective supersymmetry, Phys. Rev. Lett. 65 (1990) 2939–2942.
- [61] A. Buras, P. Gambino, M. Gorbahn, S. Jager, L. Silvestrini, Universal unitarity triangle and physics beyond the standard model, Phys. Lett. B 500 (2001) 161–167, arXiv:hep-ph/0007085.
- [62] G. D'Ambrosio, G. Giudice, G. Isidori, A. Strumia, Minimal flavor violation: an effective field theory approach, Nucl. Phys. B 645 (2002) 155–187, arXiv: hep-ph/0207036.
- [63] C. Bobeth, M. Bona, A.J. Buras, T. Ewerth, M. Pierini, et al., Upper bounds on rare K and B decays from minimal flavor violation, Nucl. Phys. B 726 (2005) 252–274, arXiv:hep-ph/0505110.
- [64] T. Hahn, Generating Feynman diagrams and amplitudes with FeynArts 3, Comput. Phys. Commun. 140 (2001) 418–431, arXiv:hep-ph/0012260.
- [65] T. Hahn, M. Perez-Victoria, Automatized one loop calculations in four and D dimensions, Comput. Phys. Commun. 118 (1999) 153–165, arXiv:hep-ph/9807565.
- [66] T. Hahn, M. Rauch, News from FormCalc and LoopTools, Nucl. Phys. B, Proc. Suppl. 157 (2006) 236–240, arXiv:hep-ph/0601248.
- [67] T. Hahn, A Mathematica interface for FormCalc-generated code, Comput. Phys. Commun. 178 (2008) 217–221, arXiv:hep-ph/0611273.
- [68] A. Denner, S. Dittmaier, M. Roth, D. Wackerlo, Predictions for all processes $e^+e^- \rightarrow$ fermions + γ , Nucl. Phys. B 560 (1999) 33–65, arXiv:hep-ph/9904472.
- [69] U. Baur, J. Vermaseren, D. Zeppenfeld, Electroweak vector boson production in high-energy ep collisions, Nucl. Phys. B 375 (1992) 3–44.
- [70] U. Baur, D. Zeppenfeld, Finite width effects and gauge invariance in radiative W productions and decay, Phys. Rev. Lett. 75 (1995) 1002–1005, arXiv:hep-ph/9503344.
- [71] M. Muhlleitner, A. Djouadi, Y. Mambrini, SDECAY: a Fortran code for the decays of the supersymmetric particles in the MSSM, Comput. Phys. Commun. 168 (2005) 46–70, arXiv:hep-ph/0311167.
- [72] M. Muhlleitner, SDECAY: a Fortran code for SUSY particle decays in the MSSM, Acta Phys. Pol. B 35 (2004) 2753–2766, arXiv:hep-ph/0409200.
- [73] A. Djouadi, M. Muhlleitner, M. Spira, Decays of supersymmetric particles: the Program SUSY-HIT (SUspect-SdecaY-Hdecay-InTerface), Acta Phys. Pol. B 38 (2007) 635–644, arXiv:hep-ph/0609292.
- [74] P.Z. Skands, B. Allanach, H. Baer, C. Balazs, G. Belanger, et al., SUSY Les Houches Accord: interfacing SUSY spectrum calculators, decay packages, and event generators, J. High Energy Phys. 0407 (2004) 036, arXiv:hep-ph/0311123.
- [75] B. Allanach, C. Balazs, G. Belanger, M. Bernhardt, F. Boudjema, et al., SUSY Les Houches Accord 2, Comput. Phys. Commun. 180 (2009) 8–25, arXiv:0801.0045 [hep-ph].
- [76] Particle Data Group, K. Olive, et al., Chin. Phys. C 38 (9) (2014) 090001.
- [77] CMS Collaboration, LHCb Collaboration, V. Khachatryan, et al., Observation of the rare $B_s^0 \rightarrow \mu^+\mu^-$ decay from the combined analysis of CMS and LHCb data, arXiv:1411.4413 [hep-ex].
- [78] S. Kraml, S. Kulkarni, U. Laa, A. Lessa, V. Magerl, W. Magerl, D. Proschofsky, M. Traub, W. Waltenberger, SMModelS v1.0: a short user guide, arXiv:1412.1745 [hep-ph].
- [79] S. Kraml, S. Kulkarni, U. Laa, A. Lessa, W. Magerl, D. Proschofsky, W. Waltenberger, SMModelS: a tool for interpreting simplified-model results from the LHC and its application to supersymmetry, Eur. Phys. J. C 74 (2014) 2868, arXiv:1312.4175 [hep-ph].
- [80] <http://smmodels.hephy.at>.
- [81] T. Sjostrand, S. Mrenna, P.Z. Skands, PYTHIA 6.4 physics and manual, J. High Energy Phys. 0605 (2006) 026, arXiv:hep-ph/0603175.
- [82] W. Beenakker, R. Hopker, M. Spira, P. Zerwas, Squark and gluino production at hadron colliders, Nucl. Phys. B 492 (1997) 51–103, arXiv:hep-ph/9610490.
- [83] W. Beenakker, M. Kramer, T. Plehn, M. Spira, P. Zerwas, Stop production at hadron colliders, Nucl. Phys. B 515 (1998) 3–14, arXiv:hep-ph/9710451.
- [84] A. Kulesza, L. Motyka, Threshold resummation for squark-antisquark and gluino-pair production at the LHC, Phys. Rev. Lett. 102 (2009) 111802, arXiv: 0807.2405 [hep-ph].
- [85] A. Kulesza, L. Motyka, Soft gluon resummation for the production of gluino-gluino and squark-antisquark pairs at the LHC, Phys. Rev. D 80 (2009) 095004, arXiv:0905.4749 [hep-ph].
- [86] W. Beenakker, S. Brensing, M. Kramer, A. Kulesza, E. Laenen, et al., Soft-gluon resummation for squark and gluino hadroproduction, J. High Energy Phys. 0912 (2009) 041, arXiv:0909.4418 [hep-ph].
- [87] W. Beenakker, S. Brensing, M. Kramer, A. Kulesza, E. Laenen, et al., Supersymmetric top and bottom squark production at hadron colliders, J. High Energy Phys. 1008 (2010) 098, arXiv:1006.4771 [hep-ph].
- [88] W. Beenakker, S. Brensing, M. Kramer, A. Kulesza, E. Laenen, et al., Squark and gluino hadroproduction, Int. J. Mod. Phys. A 26 (2011) 2637–2664, arXiv: 1105.1110 [hep-ph].
- [89] A. Buckley, PySLHA: a Pythonic interface to SUSY Les Houches Accord data, arXiv:1305.4194 [hep-ph].
- [90] CMS Collaboration, Exclusion limits on gluino and top-squark pair production in natural SUSY scenarios with inclusive razor and exclusive single-lepton searches at 8 TeV, 2014, CMS-PAS-SUS-14-011.
- [91] ATLAS Collaboration, G. Aad, et al., Search for scalar-charm pair production in pp collisions at $\sqrt{s} = 8$ TeV with the ATLAS detector, arXiv:1501.01325 [hep-ex].